Ligand Binding Is the Principal Determinant of Stability for the p21^{H-ras} Protein†

Jing Zhang and C. Robert Matthews*

Department of Chemistry and Center for Biomolecular Structure and Function, The Pennsylvania State University, University Park, Pennsylvania 16802

Received May 13, 1998; Revised Manuscript Received August 24, 1998

ABSTRACT: p21^{H-ras} is a 21 kDa, α/β sheet protein that, as a member of the GTPase superfamily, acts as a molecular switch in signal transduction pathways. The essential role of GDP and Mg^{2+} in maintaining the inactive conformation of p21^{H-ras} prompted a study of the influence of these ligands on its structure and stability. The urea-induced equilibrium unfolding transitions for the ternary (p21·GDP·Mg^{2+}), binary (p21·GDP) and apo (p21) forms of p21^{H-ras} at pH 7.5 and 25 °C were monitored by absorbance and circular dichroism spectroscopies. The cooperative disruptions of the secondary and tertiary structures for all three forms are well-described by a two-state model. Global analysis of the equilibrium unfolding data yields a free energy of folding in the absence of urea and under standard state conditions of 14.1 ± 0.2 kcal mol^{-1}, 7.5 ± 0.4 kcal mol^{-1} and 1.8 ± 0.2 kcal mol^{-1} for ternary, binary and apo forms, respectively. Near- and far-UV circular dichroism spectra of these three forms of p21^{H-ras} show that removal of the Mg^{2+} from the ternary complex loosens the aromatic side chain packing but leaves the secondary structure largely unchanged. The removal of both GDP and Mg^{2+} completely releases the side chain packing but leaves a substantial fraction of the secondary structure intact. These results demonstrate that ligands play a significant role in the stability and structure of the p21·GDP·Mg^{2+} complex. The amino acid sequence itself only contains sufficient information to direct the formation of a large portion of the secondary structure in a molten globule-like state. Ligand binding is required to drive the formation of specific tertiary structure.

The human proto-oncogene, p21^{H-ras} [1] plays a key role in intercellular signal pathways (*1*−*5*). As a molecular switch, it cycles between the GTP-bound active form and the GDP-bound inactive form through hydrolysis and ligand exchange reactions. The intrinsic conversion from the GTP-bound to GDP-bound form that accompanies hydrolysis is very slow; $k_{cat} = 0.0028$ min^{-1} (*6*). In vivo, this reaction is catalyzed by GTPase-activating proteins (GAPs) which enhance the rate by more than 10^5-fold (*7*). On the other half of the GTPase cycle, the exchange of GDP for GTP is also a slow reaction; $k_{cat} < 0.03$ min^{-1}. Guanine nucleotide exchange factors (GEFs) increase the in vivo rate by 100-fold (*4*, *8*). Point mutations at several different sites result in the disruption of the cycle and were among the first genetic lesions associated with human cancer (*2*−*4*).

p21^{H-ras} is an α/β-sheet protein with 189 amino acid residues and a molecular mass of 21 kDa. The structures of truncated p21^{H-ras} (residues 1−166) complexes with GDP and the nonhydrolyzable GTP analogues, $G_{PP}NH_P$ and $G_{PP}CH_{2P}$, have been solved to high resolution (*9*−*15*). The native conformation has five α-helices and a central β-sheet which contains five parallel and one antiparallel strands (Figure 1). Three of the loops are centered on the γ-phosphate of GTP and constitute the major portion of the active site. The side chains and backbone atoms in these loops provide a large number of polar and nonpolar interactions that stabilize the binding of the nucleotide to the protein. In the GDP-bound form, several of the loops change their orientation and their specific interactions with nucleotide and Mg^{2+}. Mg^{2+} is coordinated by the side chain hydroxyl group of Ser-17 and the β-phosphate of GDP; four water molecules complete the octahedral coordination sphere of the metal ion (*13*). Conformational changes that accompany the hydrolysis of GTP are thought to be responsible for switching this protein from the active to the inactive form (*14*, *16*, *17*).

Two features of p21^{H-ras} make it an interesting target for protein folding studies. First, an effective molecular switch must be maintained in an inactive conformation for a period that is comparable to or longer than the time required for the completion of the events stimulated by the active conformation (*4*). For switches that are driven by the binding of small molecules, a thermodynamic consequence of this temporal requirement is that these ligands must bind very tightly to either one or both of the conformations. In other words, diffusion-limited binding rates and long residence times imply large association constants. This situation is satisfied for p21^{H-ras}: the association constant for GDP in the presence of Mg^{2+} has been estimated to be in the range

† This work was supported by National Science Foundation Grant MCB 9604678 to C.R.M.

* To whom correspondence should be addressed.

[1] Abbreviations: ABS, absorbance; CD, circular dichroism; DTE, dithioerythritol; DTT, dithiothreitol; GAP, GTPase-activating protein; GDP, guanosine diphosphate; GEF, guanine nucleotide exchange factor; GTP, guanosine triphosphate; $GppCH_2p$, guanosine 5′-(β,γ-methylenetriphosphate); GppNHp, guanosine 5′-(β,γ-imidotriphosphate); IPTG, isopropyl β-D-thiogalactopyranoside; $NaDodSO_4$, sodium dodecyl sulfate; Na_2EDTA, ethylenediaminetetraacetic acid, disodium salt; PAGE, polyacrylamide gel electrophoresis; PMSF, phenylmethylsulfonyl fluoride; p21^{H-ras}, p21 protein product of the H-ras gene; Tris, tris(hydroxymethyl)aminomethane; UV, ultraviolet.

10.1021/bi9811157 CCC: $15.00
Published on Web 10/02/1998

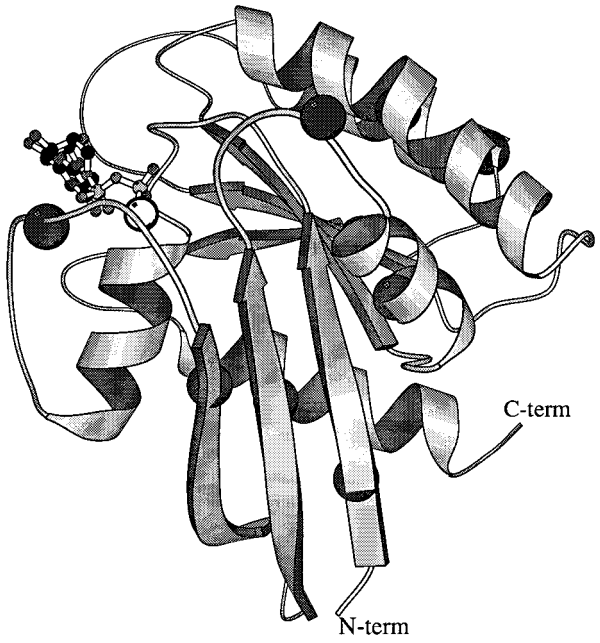

FIGURE 1: Ribbon diagram of truncated $p21^{H-ras}$ (residues 1−166) complexed with GDP and Mg^{2+} (white sphere). The positions of the nine tyrosine residues are indicated (dark spheres) (15).

of 10^7-10^{11} M^{-1} (*16*, *18*−*20*). Given the marginal stability of most proteins (*21*), the binding of these ligands should have a major impact on the stability of the ternary complex. An examination of the free energy difference between native and unfolded states of the ternary ($p21\cdot GDP\cdot Mg^{2+}$), binary ($p21\cdot GDP$), and apo (p21) forms should reveal the relative roles of the polypeptide and ligand binding on the stability and structure.

The second interesting feature of $p21^{H-ras}$ is the fact that the amino acids which comprise the guanine nucleotide binding site are highly conserved among all GTP binding proteins (*4*, *22*−*25*). Therefore, studies on $p21^{H-ras}$ may provide insight into the role of the nucleotide binding domains in the folding and stability of this class of proteins. Comparison with the folding mechanisms of proteins containing closely related domains that bind NADH or NADPH, e.g., dihydrofolate reductase (*26*−*28*), may reveal an even more general role for this very common motif.

Thermal unfolding studies on $p21^{H-ras}$ (*20*) have previously demonstrated that GDP and Mg^{2+} stabilize the protein. The melting temperature of the ternary complex of $p21^{H-ras}$ was found to be 20 °C higher than that for the apo form of the enzyme. However, the irreversibility of the thermal unfolding reaction precludes quantitative measurements of the thermodynamic properties of either species. The purpose of the present study is to determine the contribution of the ligands, GDP and Mg^{2+}, to the stability and structure of $p21^{H-ras}$ under reversible conditions.

MATERIALS AND METHODS

Protein Source and Purification. Full-length $p21^{H-ras}$ was expressed in *Escherichia coli* JM105 cells containing the TACHRAS plasmid (a gift from John H. Coulby) and purified according to previously published protocols with some modifications (*29*). Briefly, the cells were harvested 3 h after IPTG induction by centrifugation at 3300*g* at 4 °C for 30 min, and the cell paste was stored at −20 °C. Cell paste was resuspended to 0.1 g/mL with sonication buffer (20 mM Tris-HCl, pH 7.2, 100 mM NaCl, 5 mM $MgCl_2$, 1 mM DTE, and 1 mM PMSF), and the cells were washed twice after pelleting at 16000*g* for 10 min. The cells were then resuspended again to 0.1 g of cell paste/mL with sonication buffer and broken by sonication. Soluble and insoluble fractions were separated by centrifugation at 17000*g* for 30 min. If the soluble fraction was not used immediately, ammonium sulfate was added to 80%, and the resulting precipitate was stored at 4 °C.

$p21^{H-ras}$ in the soluble fraction was purified following established procedures (*29*). Purified protein was stored as a precipitate in 80% ammonium sulfate at 4 °C.

$p21^{H-ras}$ in the insoluble fraction was resuspended in the sonication buffer and pelleted at 17000*g*. The resulting pellet was resuspended with unfolding buffer (6 M urea, 20 mM Tris-HCl, pH 8.0, 50 mM NaCl, 5 mM $MgCl_2$, 30 μM GDP, 5% glycerol, 1 mM Na_2EDTA, 1 mM DTE, and 1 mM PMSF) and stirred for 1 h at 4 °C. The insoluble materials were then pelleted by centrifugation at 17000*g* for 30 min. The pellet was subjected to a second round of resuspension and centrifugation. The pooled supernatants were diluted 20-fold with dilution buffer (20 mM Tris-HCl, pH 8.0, 50 mM NaCl, 5 mM $MgCl_2$, 30 μM GDP, 5% glycerol, 1 mM DTE, and 1 mM PMSF) and incubated overnight. The sample was then loaded onto a Q-Sepharose Fast Flow anion exchange (Pharmacia) column (2.5 × 100 cm) preequilibrated at 4 °C with QFF buffer (20 mM Tris-HCl, pH 8.0, 50 mM NaCl, 5 mM $MgCl_2$, and 1 mM DTE) at a flow rate of 4 mL min^{-1}. $p21^{H-ras}$ was eluted from the column with a linear 2 L gradient from 50 to 350 mM NaCl in QFF buffer. The fractions containing $p21^{H-ras}$ were identified by $NaDodSO_4$−PAGE.

The purity of the protein was verified by the presence of a single band on Coomassie blue-stained $NaDodSO_4$−polyacrylamide gels. Protein purified from inclusion bodies was stored in 75% glycerol with 20 mM Tris-HCl, pH 7.5, 50 mM NaCl, 5 mM $MgCl_2$, 30 μM GDP, and 1 mM DTE at 4 °C.

Protein concentration was measured by the absorbance at 280 nm and calculated from Beer's Law using an extinction coefficient of 2.4×10^4 M^{-1} cm^{-1} (*30*).

Preparation of the Binary Complex, p21·GDP. The binary complex was prepared by adding 10 mM Na_2EDTA in buffer to solutions containing the ternary complex. In the presence of 1 mM $MgCl_2$ and 10 mM Na_2EDTA, the final free Mg^{2+} concentration was calculated to be about 0.1 μM from the following equation (*31*):

$$[Mg^{2+}]_{total} = [Mg^{2+}]_{free}[1 + [EDTA]_{total}/([Mg^{2+}]_{free} + K_{EDTA\cdot Mg}) + [GDP]_{total}/([Mg^{2+}]_{free} + K_{GDP\cdot Mg})] \quad (1)$$

using $K_{EDTA\cdot Mg} = 1.0 \times 10^{-6}$ M and $K_{GDP\cdot Mg} = 2.8 \times 10^{-6}$ M (*20*). At the concentrations of protein used in most of the experiments, 16 μM, the binary p21·GDP complex represented more than 97% of the protein in solution.

Preparation of Apo $p21^{H-ras}$. Apo $p21^{H-ras}$ was prepared each day by unfolding the ternary complex in a buffer containing 6 M urea, 20 mM Tris-HCl, pH 7.5 at 25 °C, 100 mM NaCl, 10 mM Na_2EDTA, and 1 mM DTT. The protein was incubated in this solution at room temperature

for 20 min. The sample was loaded onto a column of Sephadex G-25 which had been preequilibrated at 4 °C with buffer containing 6 M urea, 20 mM Tris-HCl, pH 7.5, 100 mM NaCl, and 1 mM DTT. The column was run at a flow rate of approximately 0.5 mL min^{-1}. The peak fractions were collected and assayed by UV absorbance spectroscopy.

The extinction coefficient for apo $p21^{H-ras}$ was measured by the method of Gill and von Hippel (*32*) and found to be 1.7×10^4 M^{-1} cm^{-1}.

Reagents and Experimental Conditions. Ultrapure urea was purchased from ICN Biomedical, Inc. (Costa Mesa, CA), GDP was purchased from Sigma (St. Louis, MO), and $MgCl_2$ was purchased from Aldrich Chemical Co., Inc. (Milwaukee, WI). All other chemicals were reagent grade. The buffer used in all folding experiments contained 20 mM Tris-HCl, pH 7.5, 67−100 mM NaCl, and 2 mM 2-mercaptoethanol; $MgCl_2$ and GDP concentrations were adjusted as necessary for each experiment. To maintain constant ionic strength, the concentration of NaCl was adjusted as the concentration of $MgCl_2$ or Na_2EDTA was varied. The temperature was maintained at 25 °C for all experiments.

Spectroscopic Methods. Far- and near-UV CD spectra were taken from 200 to 320 nm and from 240 to 350 nm, respectively, on an AVIV 62DS spectropolarimeter. Far-UV CD spectra were collected in 1.0 mm path length cells using a 2.0 s averaging time and a 1.0 nm step size. Near-UV CD spectra were collected in 1.0 cm cells using the same scanning parameters. The spectra reported represent the average of six repeat scans. Mean residue ellipticity was calculated using an average residue molecular mass of 112.2 g mol^{-1}. Absorbance data were collected on an AVIV 14 DS UV−Vis spectrophotometer. All samples were allowed to fully equilibrate at 25 °C before the acquisition of data.

Equilibrium Urea Titration Studies. The equilibrium unfolding reaction was monitored by CD at 222 nm and by ultraviolet absorbance spectroscopy at 287 nm. To ensure full equilibration, the ternary complex of $p21^{H-ras}$ was allowed to unfold overnight at 25 °C prior to recording the absorbance and CD spectra. The binary and apo forms of $p21^{H-ras}$ were equilibrated for 3 h before collecting the spectra. The protein concentration used in the equilibrium studies was held constant in any individual study, generally in the range of 10−17 μM.

Data Analysis. Equilibrium unfolding data for the ternary complex of $p21^{H-ras}$ were fit to the following two-state model:

$$N \overset{K}{\rightleftharpoons} U + Mg^{2+} + GDP \quad (2)$$

where N is the native ternary complex of protein, p21·Mg^{2+}·GDP, U is the unfolded form without bound ligands, and GDP and Mg^{2+} are the free ligands, respectively; $K = ([U][Mg^{2+}][GDP])/[N]$. In the presence of a significant excess of Mg^{2+} (>100 fold), the apparent fraction of the unfolded protein, F_{app}, can be shown to be

$$F_{app} = 1/2\{-([GDP]_t/[P]_t + K/([P]_t[Mg^{2+}]_t) - 1) + \{([GDP]_t/[P]_t + K/([P]_t[Mg^{2+}]_t) - 1)^2 + 4K/([P]_t[Mg^{2+}]_t)\}^{1/2}\} \quad (3)$$

where $[P]_t$, $[GDP]_t$, and $[Mg^{2+}]_t$ are the total protein, total GDP, and total Mg^{2+} concentrations, respectively.

Data from different techniques were compared by calculating the apparent fraction of unfolded protein, F_{app}, using the equation:

$$F_{app} = (Y_{obs} - Y_N)/(Y_U - Y_N) \quad (4)$$

where Y_{obs} is the observed optical parameter at a given denaturant concentration and Y_N and Y_U are the values for the native and unfolded forms under the same condition. The values of Y_N and Y_U were assumed to depend linearly on the denaturant concentration:

$$Y_N = Y_{N0} + S_N[\text{denaturant}] \quad (5a)$$

$$Y_U = Y_{U0} + S_U[\text{denaturant}] \quad (5b)$$

where Y_{N0} and Y_{U0} are the values in the absence of denaturant and S_N and S_U are the slopes of the native and unfolded base line regions, respectively. The equilibrium constant, K, from eq 2 can be written as $K = \exp[-(\Delta G°/RT)]$, where $\Delta G°$ is the free energy difference between the native and unfolded forms at a given denaturant concentration. The urea dependence of $\Delta G°$ was assumed to have a linear dependence on the denaturant concentration (*33*): $\Delta G° = \Delta G°(H_2O) - m[\text{urea}]$. $\Delta G°(H_2O)$ is the free energy difference in the absence of denaturant, and m reflects the sensitivity of the unfolding transition to denaturant.

Combining eqs 3−5, Y_{obs} can be calculated as

$$Y_{obs} = 1/2\{(Y_{U0} - Y_{N0}) + (S_N - S_U)[\text{urea}]\}\{-([GDP]_t/[P]_t + \exp(-(\Delta G°(H_2O) - m[\text{urea}])/RT)/([P]_t[Mg^{2+}]_t) - 1) + \{([GDP]_t/[P]_t + \exp(-(\Delta G°(H_2O) - m[\text{urea}])/RT)/([P]_t[Mg^{2+}]_t) - 1)^2 + 4\exp(-(\Delta G°(H_2O) - m[\text{urea}])/RT)/([P]_t[Mg^{2+}]_t)\}^{1/2} + Y_{N0} + S_{N0}[\text{urea}] \quad (6)$$

This equation was used to fit the observed data using Savuka, version 5.1, an in-house global fitting program.

When Mg^{2+} is removed from the ternary complex by adding excess Na_2EDTA to the buffer solution, the equilibrium unfolding reaction for the binary complex can be written as

$$N \overset{K}{\rightleftharpoons} U + GDP \quad (7)$$

where $K = ([U][GDP])/[N]$ and N is the native binary complex, p21·GDP. F_{app} can be expressed as

$$F_{app} = 1/2\{([GDP]_t/[P]_t + K/[P]_t - 1) + \{([GDP]_t/[P]_t + K/[P]_t - 1)^2 + 4K/[P]_t\}^{1/2}\} \quad (8)$$

Assuming that the baseline regions depend linearly on the denaturant concentration, the observed signal, Y_{obs}, can be calculated as

$$Y_{obs} = 1/2\{(Y_{U0} - Y_{N0}) + (S_N - S_U)[\text{urea}]\}\{-([\text{GDP}]_t/[\text{P}]_t + \exp(-(\Delta G°(\text{H}_2\text{O}) - m[\text{urea}])/RT)/[\text{P}]_t - 1) + \{([\text{GDP}]_t/[\text{P}]_t + \exp(-(\Delta G°(\text{H}_2\text{O}) - m[\text{urea}])/RT)/[\text{P}]_t - 1)^2 + 4\exp(-(\Delta G°(\text{H}_2\text{O}) - m[\text{urea}])/RT)/[\text{P}]_t\}^{1/2} + Y_{N0} + S_{N0}[\text{urea}] \quad (9)$$

Equation 9 was used to fit the equilibrium data from the binary form using Savuka, version 5.1.

The equilibrium folding reaction of apo $p21^{H-ras}$ was fit to a two-state model:

$$N \overset{K}{\rightleftharpoons} U \quad (10)$$

where K= [U]/[N], N is the native apoprotein, and $F_{app} = K/(1 + K)$. Y_{obs} can be calculated as

$$Y_{obs} = \{(Y_{U0} - Y_{N0}) + (S_N - S_U)[\text{urea}]\}\{\exp(-(\Delta G°(\text{H}_2\text{O}) - m[\text{urea}])/RT))/(1 + \exp(-(\Delta G°(\text{H}_2\text{O}) - m[\text{urea}])/RT)\} + Y_{N0} + S_{N0}[\text{urea}] \quad (11)$$

This equation was used to fit the observed data using Savuka, version 5.1.

RESULTS

Secondary Structure in Ternary, Binary, and Apo $p21^{H-ras}$. The far-UV CD spectra of the native ternary and fully unfolded conformations of $p21^{H-ras}$ are shown in Figure 2. The spectrum of the ternary complex exhibits a broad minimum near 220 nm, typical of α/β-sheet proteins. The ellipticity at 222 nm is dramatically reduced in the presence of 8 M urea, indicating that little or no secondary structure remains under these conditions. The mean residue ellipticity at 222 nm of the ternary complex is -12.3×10^3 deg cm^2 dmol^{-1}, and that for the unfolded form is -2.0×10^3 deg cm^2 dmol^{-1}. The far-UV CD spectra of $p21^{H-ras}$ in the binary and apo forms are also shown in Figure 2. The mean residue ellipticity at 222 nm of the binary complex is -12.1×10^3 deg cm^2 dmol^{-1}, and that for the apo protein is -9.51×10^3 deg cm^2 dmol^{-1}.

The observed changes in the shape of the spectra and the position of the minima suggest that the removal of Mg^{2+} to form the binary complex causes small perturbations in the secondary and, possibly, tertiary structure (*34*). The removal of GDP and Mg^{2+} to form the apo protein induces a somewhat larger decrease in the ellipticity at 222 nm and a shift of the minimum to 213 nm. Even with these changes, it is evident that the apo protein has significant secondary structure. Perturbations in the secondary structure of the binary and apo forms might be expected because both ligands directly contact the loops which link the helices and strands that define the native conformation (Figure 1).

Tertiary Structure in Ternary, Binary, and Apo $p21^{H-ras}$. Near-UV CD spectroscopy was used to examine the chirality of the environments of the nine tyrosines and five phenylalanines in $p21^{H-ras}$; this protein lacks tryptophan. The ternary complex, p21·GDP·Mg^{2+}, shows a strong positive signal near 287 nm (Figure 3) which primarily reflects the tyrosine side chain packing in the native conformation. When the Mg^{2+} is removed to form the binary complex, the amplitude of the signal at 287 nm is decreased by about 15%. When both GDP and Mg^{2+} are removed to form the apo

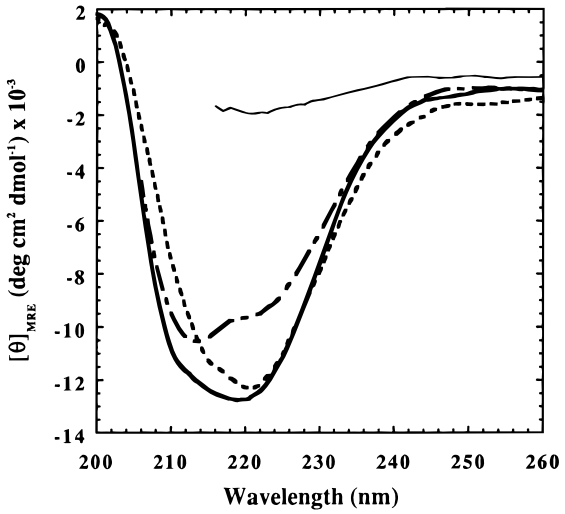

FIGURE 2: Far-UV CD spectra of $p21^{H-ras}$. The thick solid line shows the spectrum of the native ternary complex, and the thin solid line represents the spectrum of the fully unfolded conformation in 8 M urea. The short dashed line shows the spectrum of the binary complex, and the alternating long and short dashes show the spectrum of the apo protein. The protein concentration was 16 μM for both ternary and binary complexes as well as for the unfolded protein and 10 μM for the apo protein. The buffer used for the ternary complex contained 20 mM Tris-HCl, pH 7.5, 85 mM NaCl, 10 μM GDP, 5 mM Mg^{2+}, 0.6 M urea, and 2 mM 2-mercaptoethanol. The buffer used for the binary complex contained 20 mM Tris-HCl, pH 7.5, 67 mM NaCl, 10 μM GDP, 1 mM Mg^{2+}, 10 mM Na_2EDTA, 0.6 M urea, and 2 mM 2-mercaptoethanol. The total GDP concentration in the solutions of ternary and binary complexes was 26 μM. The buffer used for the apo protein contained 20 mM Tris-HCl, pH 7.5, 100 mM NaCl, 0.6 M urea, and 2 mM 2-mercaptoethanol. The 0.6 M urea required to maintain the apo protein in a soluble form was also included in the solutions for the ternary and binary complexs. All spectra were taken at 25 °C.

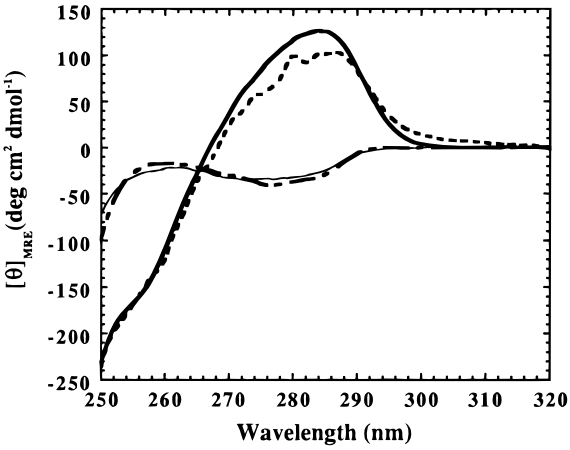

FIGURE 3: Near-UV CD spectra of $p21^{H-ras}$. The thick solid line shows the spectrum of the native ternary complex; the thin solid line represents the spectrum of the fully unfolded conformation in 8 M urea. The short dashed line shows the spectrum of the binary complex, and the alternating long and short dashes show the spectrum of the apo protein. The final protein concentration was 70 μM. The buffers used for the three forms of $p21^{H-ras}$ are described in the caption for Figure 2.

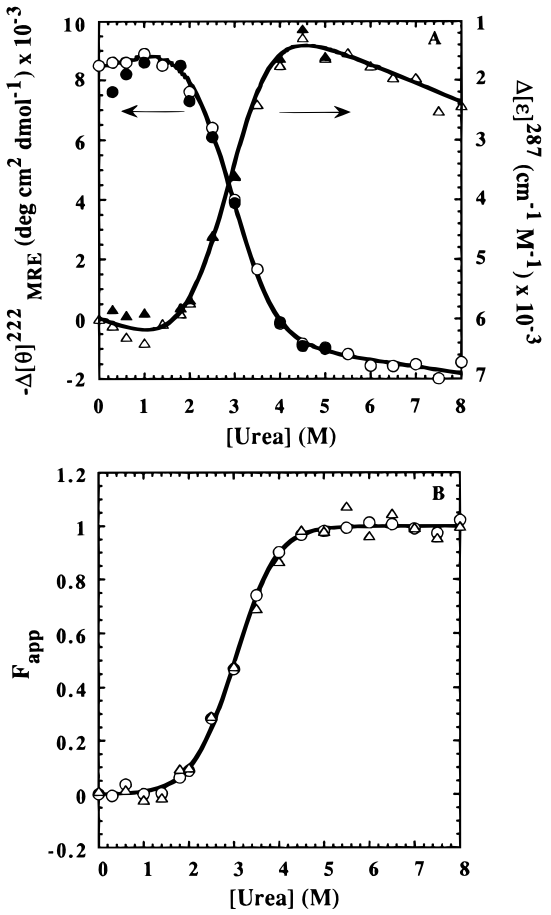

FIGURE 4: Equilibrium unfolding of the ternary complex of p21^{H-ras}. (A) Dependence of the mean residue ellipticity at 222 nm (○) and the extinction coefficient at 287 nm (△) on the urea concentration. Closed symbols represent the results for refolded protein that had previously been unfolded in 6 M urea. (B) The apparent fraction of unfolded protein, F_{app}, versus the urea concentration. The line represents the simultaneous global fits of both the CD and ABS data to eq 6. The protein concentration was 16.5 μM, and the total GDP concentration was 17.5 μM. Buffer conditions: 20 mM Tris-HCl, pH 7.5, 85 mM NaCl, 5 mM $MgCl_2$, 1.0 μM GDP, and 2 mM 2-mercaptoethanol at 25 °C.

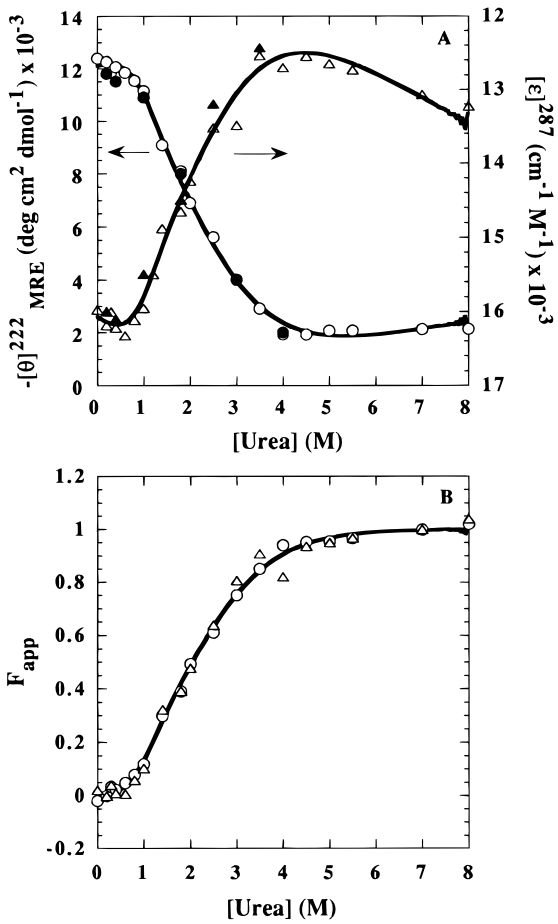

FIGURE 5: Equilibrium unfolding of the binary complex of p21^{H-ras}. (A) Dependence of the mean residue ellipticity at 222 nm (○) and the extinction coefficient at 287 nm (△) on the urea concentration. Closed symbols represent the results of refolding protein that had previously been unfolded in 6 M urea. (B) The apparent fraction of unfolded protein, F_{app}, versus the urea concentration. Lines represent the global fits of both the CD and ABS data to eq 9. The protein concentration was 16 μM, and the total GDP concentration was 26 μM. Buffer conditions: 20 mM Tris-HCl, pH 7.5, 67 mM NaCl, 1 mM $MgCl_2$, 10 mM Na_2EDTA, 10 μM GDP, and 2 mM 2-mercaptoethanol at 25 °C.

protein, a broad, slightly negative signal is observed in this region. The near-UV CD spectrum of apo p21 is very similar to the spectrum of the unfolded ternary complex (Figure 3), demonstrating that the packing around the aromatic side chains is completely disrupted in the absence of both ligands.

Stability of Ternary, Binary, and Apo p21^{H-ras}. Urea titration experiments were performed to determine the appropriate folding models and stabilities of the ternary, binary, and apo forms of p21^{H-ras}. The changes in extinction coefficient at 287 nm and mean residue ellipticity at 222 nm for the ternary complex of p21^{H-ras} as a function of urea concentration are presented in Figure 4A. As the urea concentration is increased, the CD and UV absorbance signals change in a sigmoidal fashion, indicative of cooperative unfolding transitions. The reversibility of the unfolding reaction was demonstrated by unfolding the protein overnight in 6 M urea followed by refolding by dilution into buffer. By comparing the spectrum of refolded protein to that obtained from unfolding the native protein under the same final conditions, it was demonstrated that the urea-induced equilibrium unfolding reaction of p21^{H-ras} is greater than 90% reversible.

The fits of the equilibrium data, generated by ABS and CD spectroscopy, to a two-state model that incorporates both the protein and ligand concentrations (eq 6) are shown in Figure 4 as solid lines. The coincidence of the normalized, F_{app}, curves for both techniques (Figure 4B) and the excellent agreement with the predicted curve for a two-state model demonstrate that only the native, ternary complex and the unfolded, ligand-free form are highly populated at equilibrium during urea-induced unfolding.

The same experiments were performed on the p21·GDP binary complex and the apo protein. The results are shown in Figure 5 and Figure 6, respectively. Removal of Mg^{2+} to form the binary complex appears to destabilize the protein as evidenced by the ~1 M urea shift in the midpoint of the unfolding transition to lower urea (Figure 5). In addition, the unfolding transition occurs over a broader urea range, indicative of a decrease in the amount of surface area buried (*35*) relative to the ternary complex. Removal of both ligands to form the apo protein results in an additional loss of stability as evidenced by the absence of a well-defined native baseline region and an even broader transition zone (Figure 6). Removal of ligands did not have a detrimental

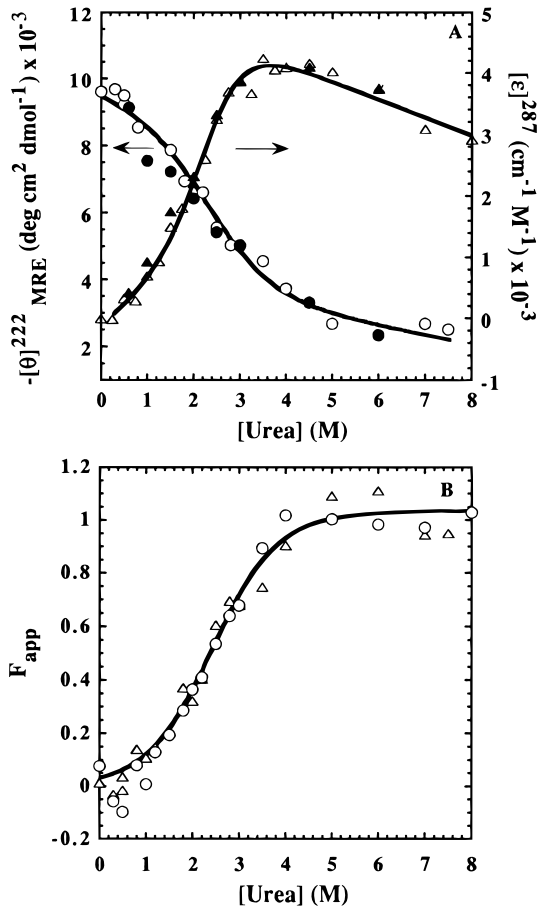

FIGURE 6: Equilibrium unfolding of the apo form of p21^{H-ras}. (A) Dependence of the mean residue ellipticity at 222 nm and the extinction coefficient at 287 nm on the urea concentration, as measured by CD (○) and by ABS (△), respectively. (B) The apparent fraction of unfolded protein, F_{app}, versus the urea concentration. Closed symbols represent refolding points. Lines represent the global fit of both the CD and ABS data to eq 11. The protein concentration was 10 μM. Buffer conditions: 20 mM Tris-HCl, pH 7.5, 100 mM NaCl, 2 mM 2-mercaptoethanol at 25 °C.

effect on the reversibility of the unfolding transition as can be seen by the near-coincidence of the solid and open symbols in Figures 5A and 6A. The solid lines represent fits of the binary and apo unfolding data to the appropriate two-state models, using eqs 9 and 11, respectively. The coincidence of the normalized CD and ABS unfolding curves suggests that both the binary and apo proteins are also well described by a two-state equilibrium unfolding transition (Figures 5B and 6B). The two-state model is also consistent with the decreased stability of the binary and apo forms relative to the ternary form (Table 1); these species are expected to be only marginally populated in the equilibrium unfolding of the ternary complex.

As a further test of the two-state model for the ternary and binary forms of p21^{H-ras}, the effect of varying the concentrations of these ligands on the apparent stabilities was measured. When the total GDP concentration was increased from 17.5 to 112.5 μM and the $MgCl_2$ and protein concentrations were maintained constant at 5 mM and 12.5 μM, respectively, the midpoint of the unfolding transition for the ternary complex monitored by CD spectroscopy increased from 3.1 M urea to 4.0 M urea (Figure 7A). When the total concentration of Mg^{2+} was increased from 0.1 μM to 5 mM and the total GDP and protein concentrations were held constant at 27 and 17 μM, respectively, the midpoint of the unfolding transition increased from 2.0 to 3.5 M urea (Figure 7B). These results are consistent with the dissociation of both ligands from the protein as it unfolds. The effect of GDP binding on the apparent stability of the binary complex, p21·GDP, was tested by repeating the urea titration at several different GDP concentrations. As expected, the midpoint of the unfolding transition increased with increasing GDP concentration (data not shown). Attempts to study the effect of Mg^{2+} on the stability of the apo form were precluded by problems with aggregation.

The thermodynamic parameters were extracted from the fits of the data to appropriate two-state models as described under Materials and Methods.

Table 1 shows the results from both global and individual fits of a series of equilibrium unfolding experiments for the ternary and binary complexes. For the individual fits, the consistency in the values obtained for the thermodynamic parameters over a wide range of ligand concentrations supports the simplified two-state equilibrium models presented in eqs 2 and 7 for the ternary and binary complexes, respectively. For the ternary complex, a global fit of 11 data sets obtained from equilibrium CD and ABS experiments over a range of ligand and protein concentrations gave a free energy change under standard state conditions and in the absence of urea of 14.1 ± 0.2 kcal mol^{-1} and an *m* value of 1.37 ± 0.05 kcal mol^{-1} (molar urea)$^{-1}$. For the binary complex, a global fit of 6 data sets over a range of GDP and protein concentrations results in corresponding values of 7.5 ± 0.4 kcal mol^{-1} and 1.0 ± 0.1 kcal mol^{-1} (molar urea)$^{-1}$, respectively. The results of the global fits are consistent with those of the individual fits (Table 1), providing further support for the validity of a two-state model for the ternary and binary complexes of p21^{H-ras} protein. Although the marginal stability of the apo protein precluded a well-defined native baseline, the transitions were sufficiently complete to provide reliable fits. A combined fit of the ABS and CD data shown in Figure 6 for the apo protein yielded a free energy of unfolding in the absence of urea under standard state conditions of 1.8 ± 0.2 kcal mol^{-1} and an *m* value of 0.78 ± 0.02 kcal mol^{-1} (molar urea)$^{-1}$, respectively.

DISCUSSION

Stability and Structure of Apo p21^{H-ras} and Its Binary and Ternary Complexes with GDP and Mg^{2+}. Thermodynamic studies on the urea-induced unfolding of apo p21^{H-ras} and its binary and ternary complexes with GDP and GDP/Mg^{2+}, respectively, have shown that these ligands have a substantial influence on the stability and the nature of side chain packing. Interestingly, the secondary structure is less influenced by these ligands than is the tertiary structure.

In the presence of both GDP and Mg^{2+}, the free energy of folding in the absence of denaturant is 14.1 ± 0.2 kcal mol^{-1}. This value is comparable to that of many small, globular proteins (*21*) and reflects the numerous noncovalent interactions observed in the X-ray structure (*11*) and implied by the near- and far-UV CD spectra (Figures 2 and 3). Removal of the Mg^{2+} decreases the stability by nearly half to 7.5 ± 0.4 kcal mol^{-1}. The binding of this doubly charged cation to the β-phosphate of GDP and the hydroxyl of Ser17

Table 1: Stability Parameters for the Unfolding of P21^{H-ras} as a Function of Ligand Concentration at pH 7.5 and 25 °C

	[GDP][a] (μM)	[Mg^{2+}][a] (mM)	[P] (μM)	$\Delta G°(H_2O)$ (kcal mol^{-1})	m [kcal mol^{-1} (molar urea)$^{-1}$]	C_m[b](M)	technique
				Ternary Complex			
individual fits	17.5	5.00	12.5	13.7 ± 0.7	1.36 ± 0.2	3.0	CD
	17.5	5.00	16.5	14.0 ± 0.3	1.34 ± 0.1	3.0	CD
	23.6	5.00	12.5	13.5 ± 0.5	1.30 ± 0.2	3.2	CD
	37.4	5.00	12.5	14.0 ± 0.2	1.38 ± 0.1	3.5	CD
	112.5	5.00	12.5	13.9 ± 0.5	1.37 ± 0.1	4.0	CD
	27.0	1.02	17.0	14.0 ± 0.4	1.34 ± 0.06	2.8	CD
	27.0	5.02	17.0	14.0 ± 0.2	1.39 ± 0.05	3.4	CD
	23.65	5.00	12.5	14.1 ± 0.5	1.33 ± 0.2	3.2	ABS
	27.06	1.02	17.0	14.6 ± 0.4	1.41 ± 0.1	2.7	ABS
	27.0	5.02	17.0	14.5 ± 0.5	1.39 ± 0.1	3.3	ABS
	37.4	5.00	12.5	14.2 ± 0.5	1.33 ± 0.2	3.4	ABS
global fit[c]				14.1 ± 0.2	1.37 ± 0.05		
				Binary Complex			
individual fits	22.0	0.001	13.5	7.6 ± 0.3	1.1 ± 0.2	1.4	CD
	26.0	0.001	13.5	7.6 ± 0.3	1.0 ± 0.2	1.4	CD
	100.0	0.001	13.5	7.6 ± 0.2	0.99 ± 0.3	2.2	CD
	27.0	0.001	17.0	7.7 ± 1.0	0.98 ± 0.1	1.4	CD
	26.0	0.001	13.5	7.5 ± 0.8	1.1 ± 0.2	1.4	ABS
	27.0	0.001	17.0	7.4 ± 0.9	0.95 ± 0.3	1.4	ABS
global fit[d]				7.5 ± 0.4	1.0 ± 0.1		

[a] [GDP] and [Mg^{2+}] are the total concentrations. Errors in the protein concentration are ±10%. [b] The midpoint of the unfolding transition was calculated from the F_{app} equations at the urea concentration where $F_{app} = 0.5$. Errors in C_m are estimated to be ±0.06 M. [c] The global fit included all 11 data sets shown. [d] The global fit included all 6 data sets shown.

as well as its involvement in a network of water-mediated hydrogen bonds to other side chains (*17*) appears to contribute significantly to the free energy of folding of the ternary complex. This substantial decrease in stability is accompanied by relatively modest changes in both the far- and near-UV CD spectra (Figures 2 and 3), suggesting that both the secondary and tertiary structures are largely intact in the binary complex. The decrease in the m value from 1.38 to 1.0 kcal mol^{-1} M^{-1}, however, indicates that the amount of buried surface area (*35*) decreases when the Mg^{2+} is removed to form the binary complex. This result may reflect, in part, the release of Ser17 and the dissociation of helix α1 which contains this residue.

When the GDP is removed to create apo p21^{H-ras}, the stability undergoes a further decrease to 1.8 ± 0.2 kcal mol^{-1}. The marginal stability of apo p21^{H-ras} leads to the prediction that this form of the protein is approximately 5% unfolded in the absence of denaturant (Figure 6). Therefore, the ellipticity at 222 nm for the fully folded apo form should be approximately 5% greater than that shown in Figure 2. Including this correction, the ellipticity at 222 nm for the apo protein is predicted to be about 80% that of the ternary complex. Although there are obvious differences in the far-UV CD spectra of ternary and apo p21^{H-ras} (Figure 2), the substantial amount of remaining secondary structure is in striking contrast to the complete loss of specific side chain packing around the aromatic chromophores in the apo protein (Figure 3).

The numerous polar and nonpolar contacts between GDP and the protein not only promote ligand binding at the active site but also serve to organize the aromatic and, presumably, other side chains in the protein. The loss of side chain packing and further reduction in secondary structure observed for the apo form are also consistent with the observed decrease in the m value for the urea-induced unfolding transition, relative to the binary complex. Presumably, the decrease in organized structure allows greater solvent access to surface area that is buried in the binary form of p21^{H-ras}.

Nativelike secondary structure and the absence of fixed tertiary structure are characteristics of the molten globule state, an often-observed early intermediate in folding reactions (36−38). For a number of proteins, these alternatively folded states are only stable under extreme conditions, i.e., low pH or high temperature, which selectively destabilize the native conformation. However, ligands play such a critical role in stabilizing the native conformation of p21^{H-ras} that their removal offers access to a molten globule-like state at neutral pH and 25 °C.

Similar results have been obtained by Shortle and his colleagues on a truncated version of staphylococcal nuclease. This reduced polypeptide adopts a partially folded form that packs elements of secondary structure in a nativelike fashion (*39*, *40*) but lacks specific tertiary structure. This conformer can be converted to a nativelike conformation by the addition of nucleotide and calcium (*41*, *42*). As another example, α-lactalbumin exhibits a molten globule state simply by removing Ca^{2+} at neutral pH (*43*, *44*). Evidence has been presented that apo α-lactalbumin can adopt a nativelike chain fold in the α-domain but not the β-domain (*45*). This latter conclusion, however, has been disputed (*46*).

A common theme in these examples is that the amino acid sequences of these apo or truncated proteins only contain enough information and intrinsic folding energy to drive the folding reaction to a molten globule-like stage. The driving force to complete the folding reaction requires the binding of ligand(s) to the native conformation. This phenomenon might be regarded as a corollary of the Anfinsen hypothesis (*47*) in that part of the information required to fold to the native conformation may be contained in factors extrinsic to the amino acid sequence. If the binding of these factors

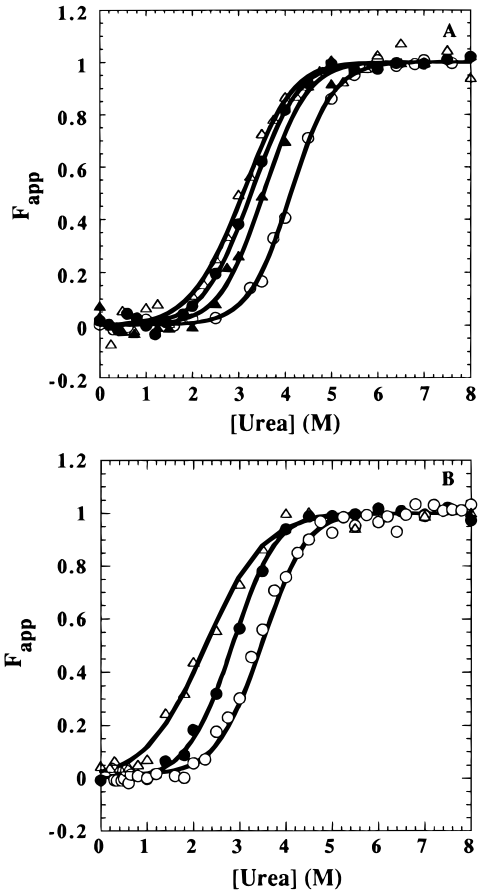

FIGURE 7: Effect of ligand concentrations on the apparent fraction of unfolded protein, F_{app}, versus the urea concentration for the ternary complex. Data are from equilibrium CD studies at 222 nm. (A) Effect of GDP concentration on the equilibrium unfolding reaction. The total GDP concentration was 17.5 (open triangles), 23.5 (closed circles), 37.4 (closed triangles), and 112.5 μM (open circles), respectively. The protein and Mg^{2+} concentrations were 12.5 μM and 5 mM, respectively. (B) Effect of Mg^{2+} concentration on the equilibrium unfolding reaction. The final Mg^{2+} concentration was 0.1 μM (open triangles), 1 mM (closed circles), and 5 mM (open circles), and the total GDP and protein concentrations were 27 and 17 μM, respectively. Lines represent the global fits of these data to eq 3 except for the fit in panel (B) with a Mg^{2+} concentration of 0.1 μM. In this case, the data were fit by eq 9.

provides the energy required to stabilize a unique, native fold that is thermodynamically and structurally different from the dynamic ensemble of partially folded forms that exist in the absence of ligands, then the ligands themselves contain essential folding information. A related situation exists for the tryptophan repressor, a dimeric protein whose individual subunits are highly intertwined. Polar mutations in the hydrophobic core preclude the formation of the dimer but not the folding of the individual subunits to non-native conformations (*48*). Thus, a part of the information required to direct the correct folding of one of the tryptophan repressor subunits is contained in the other subunit.

Relationship between Ligand Affinity and Protein Stability. The reported association constant of GDP for $p21^{H-ras}$ in the presence of millimolar concentrations of magnesium ranges from 1.7×10^7 (*18*) to $(2.1-5.7) \times 10^{10}$ M^{-1} (*16*, *19*, *20*) under conditions similar to those in the present experiments. These values correspond to a range in the free energy of binding from 9.6 to 14.7 kcal mol^{-1}. If the predominant, folded apo enzyme is the species to which the ligands bind, the difference in stability between the ternary and apo forms of $p21^{H-ras}$, 12.3 kcal mol^{-1}, reflects the binding free energy of the ligands. This corresponds to an association constant for GDP of 1×10^9 M^{-1} at pH 7.5, 25 °C, and excess Mg^{2+}, within the range of previous measurements. If the ligands instead bind to a minor conformer in equilibrium with the predominant conformer, the binding free energy estimated by this approach would increase in direct proportion to the difference in free energy between the two conformers. In effect, the binding energy would be decreased by the energy required to convert the stable apo form to the minor, ligand-competent form. Therefore, an association constant of 1×10^9 M^{-1} represents a lower limit for this parameter.

Biological Implications. The observation that the stability of the ternary complex of $p21^{H-ras}$ is dominated by the binding of GDP and Mg^{2+} may reflect both general aspects of enzyme function and turnover and specific aspects of the function of this protein. As discussed above, tight ligand binding can be a thermodynamic consequence of slow ligand release. However, strong binding to a very stable apo protein would result in a complex whose stability could exceed 20 kcal mol^{-1} at standard state. A stability of this magnitude for an enzyme could be detrimental to catalysis or to proteolytic turnover by reducing access to small populations of essential high-energy states. These and other reasons might explain the observed marginal stability of many globular proteins, 5−15 kcal mol^{-1} (*21*).

For $p21^{H-ras}$, the rates of turnover of GTP to GDP and exchange of GDP for GTP, in the absence of other cellular factors, might be significantly retarded if the stability of the ternary complex exceeded 20 kcal mol^{-1}. For example, the exchange reaction for the GDP ternary complex might be mediated through binding of GEF to a partially unfolded form of the complex that has a lower affinity for ligands. Extraordinary stability of the ternary complex could reduce the population of an exchange-competent state, thereby inhibiting the action of GEF. Although the catalytic power of GAPs (*7*, *49*) and GEFs (*4*, *8*) could be adjusted by mutations to overcome this additional retardation, the primitive signaling system that might have existed before GAPs and GEFs evolved might not have been useful on a biological time scale. Therefore, the marginal stability of the apo form of $p21^{H-ras}$ might be a necessary consequence of the tight binding of the GDP and Mg^{2+} ligands.

ACKNOWLEDGMENT

We are grateful to Dr. S. Campbell-Burk for the gift of the gene for $p21^{H-ras}$ and the purification protocol for this protein. We thank Drs. J. A. Zitzewitz and V. F. Smith for their critical reviews of the manuscript and S. A. Wasta for her assistance with references. We also thank Drs. D. Lambright and O. Bilsel for the development of Savuka 5.1, an in-house global fitting program.

APPENDIX

Derivation of Equation 3. From the expression for the equilibrium constant

$$K = ([U][Mg^{2+}][GDP])/[N] \qquad (A1)$$

we seek an expression for [U] in terms of the following known quantities: the total protein concentration, P_t, the total magnesium ion concentration, $[Mg^{2+}]_t$, and the total GDP concentration, $[GDP]_t$. Mass balance yields

$$[Mg^{2+}]_t = [Mg^{2+}] + [N] \quad \text{(A2)}$$

$$[GDP]_t = [GDP] + [N] \quad \text{(A3)}$$

$$[N] = P_t - [U] \quad \text{(A4)}$$

Rearranging and substituting into eq A1 yield

$$K = \{[U]([Mg^{2+}]_t - P_t + [U])([GDP]_t - P_t + [U])\}/(P_t - [U]) \quad \text{(A5)}$$

The cubic equation in [U] can be reduced to a quadratic equation if we take $[Mg^{2+}]_t \gg P_t$, which is a good approximation for the conditions of these experiments. Then eq A2 simplifies to

$$K = \{[U][Mg^{2+}]_t([GDP]_t - P_t + [U])\}/(P_t - [U]) \quad \text{(A6)}$$

Rearranging yields a quadratic equation in terms of [U]:

$$-[U]^2 + A[U] + P_tK/[Mg^{2+}]_t = 0 \quad \text{(A7)}$$

whose solution is

$$[U] = 1/2\{-A + (A^2 + (4KP_t/[Mg^{2+}]_t))^{1/2}\} \quad \text{(A8)}$$

where

$$A = [GDP]_t + (K/[Mg^{2+}]_t) - P_t \quad \text{(A9)}$$

The apparent fraction unfolded protein is then given by

$$F_{app} = [U]/P_t \quad \text{(A10)}$$

A similar method can be used to derive eq 8.

REFERENCES

1. Bar-sagi, D., and Feramisco, J. R. (1985) *Cell 42*, 841−848.
2. Barbacid, M. (1987) *Annu. Rev. Biochem. 56*, 779−827.
3. Bourne, H. R., Sanders, D. A., and McCormick, F. (1990) *Nature 348*, 125−132.
4. Bourne, H. R., Sanders, D. A., and McCormick, F. (1991) *Nature 349*, 117−127.
5. Hall, A. (1994) *Science 264*, 1413−1414.
6. Temeles, G. L., Gibbs, J. B., D'Alonzo, J. S., Sigal, I. S., and Scolnick, E. M. (1985) *Nature 313*, 700−703.
7. Gideon, P., John, J., Frech, M., Lautwein, A., Clark, R., Scheffler, J. E., and Wittinghofer, A. (1992) *Mol. Cell. Biol. 12*, 2050−2054.
8. Mosteller, R. D., Han, J., and Broek, D. (1994) *Mol. Cell. Biol. 14*, 1104−1112.
9. De Vos, A. M., Tong, L., Milburn, M. V., Matias, P. M., Jancarik, J., Noguchi, S., Nishimura, S., Miura, K., Ohtsuka, E., and Kim, S.-H. (1988) *Science 239*, 888−893.
10. Milburn, M. V., Tong, L., de Vos, A. M., Brunger, A., Yamaizumi, Z., Nishimura, S., and Kim, S.-H. (1990) *Science 247*, 939−945.
11. Pai, E. F., Krengel, U., Petsko, G. A., Goody, R. S., Kabsch, W., and Wittinghofer, A. (1990) *EMBO J. 9*, 2351−2359.
12. Schlichting, I., Almo, S. C., Rapp, G., Wilson, K., Petratos, K., Lentfer, A., Wittinghofer, A., Kabsch, W., Pai, E. F., Petsko, G. A., and Goody, R. S. (1990) *Nature 345*, 309−315.
13. Tong, L., de Vos, A. M., Milburn, M. V., and Kim, S. H. (1991) *J. Mol. Biol. 217*, 503−516.
14. Goody, R. S., Pai, E. F., Schlichting, I., Rensland, H., Scheidig, A., Franken, S., and Wittinghofer, A. (1992) *Philos. Trans. R. Soc. London 336*, 3−10.
15. Kraulis, P. J., Domaille, P. J., Campbell-Burk, S. L., Van Aken, T., and Laue, E. D. (1994) *Biochemistry 33*, 3515−3531.
16. Feuerstein, J., Kalbitzer, H. R., John, J., Goody, R. S., and Wittinghofer, A. (1987) *Eur. J. Biochem. 162*, 49−55.
17. Wittinghofer, A., Franken, S. M., Scheidig, A. J., Rensland, H., Lautwein, A., Pai, E. F., and Goody, R. S. (1993) *The GTPase Superfamily*, Wiley, Chichester.
18. Manne, V., Bekesi, E., and Kung, H.-F. (1985) *Proc. Natl. Acad. Sci. U.S.A. 82*, 376−380.
19. John, J., Sohmen, R., Feuerstein, J., Linke, R., Wittinghofer, A., and Goody, R. S. (1990) *Biochemistry 29*, 6058−6065.
20. Mistou, M.-Y., Cool, R. H., and Parmeggiani, A. (1992) *Eur. J. Biochem. 204*, 179−185.
21. Pace, C. N. (1975) *Crit. Rev. Biochem. 3*, 1−43.
22. Halliday, K. R. (1983) *J. Cyclic Nucleotide Protein Phosphorylation Res. 9*, 435−448.
23. McCormick, F., Clark, B. F. C., LaCour, T. F. M., Kjeldgaard, M., Norskov-Lauritsen, L., and Nyborg, J. (1985) *Science 230*, 78−82.
24. Dever, T. E., Glynias, M. J., and Merrick, W. C. (1987) *Proc. Natl. Acad. Sci. U.S.A. 84*, 1814−1818.
25. Valencia, A., Kjeldgaard, M., Pai, E. F., and Sander, C. (1991) *Proc. Natl. Acad. Sci. U.S.A. 88*, 5443−5447.
26. Touchette, N. A., Perry, K. M., and Matthews, C. R. (1986) *Biochemistry 25*, 5445−5452.
27. Ahrweiler, P. M., and Frieden, C. (1991) *Biochemistry 30*, 7801−7809.
28. Jennings, P. A., Finn, B. E., Jones, B. E., and Matthews, C. R. (1993) *Biochemistry 32*, 3783−3789.
29. DeLoskey, R. J., Van Dyk, D. E., Van Aken, T. E., and Campbell-Burk, S. (1994) *Arch. Biochem. Biophys. 311*, 72−78.
30. Moore, K. J. M., Webb, M. R., and Eccleston, J. F. (1993) *Biochemistry 32*, 7451−7459.
31. Higashijima, T., Ferguson, K. M., Smigel, M. D., and Gilman, A. G. (1987) *J. Biol. Chem. 262*, 757−761.
32. Gill, S. C., and von Hippel, P. H. (1989) *Anal. Biochem. 182*, 319−326.
33. Santoro, M. M., and Bolen, D. W. (1988) *Biochemistry 27*, 8063−8068.
34. Kuwajima, K., Garvey, E. P., Finn, B. E., Matthews, C. R., and Sugai, S. (1991) *Biochemistry 30*, 7693−7703.
35. Myers, J. K., Pace, C. N., and Scholtz, J. M. (1995) *Protein Sci. 4*, 2138−2148.
36. Kuwajima, K. (1989) *Proteins: Struct., Funct., Genet. 6*, 87−103.
37. Fink, A. L. (1995) *Annu. Rev. Biophys. Biomol. Struct. 24*, 495−522.
38. Ptitsyn, O. B. (1995) *Adv. Protein Chem. 47*, 83−229.
39. Alexandrescu, A. T., Gittis, A. G., Abeygunawardana, C., and Shortle, D. (1995) *J. Mol. Biol. 250*, 134−143.
40. Shortle, D. (1996) *Curr. Opin. Struct. Biol. 6*, 24−30.
41. Shortle, D., and Abeygunawardana, C. (1993) *Structure 1*, 121−134.
42. Shortle, D. (1996) *FASEB 10*, 27−34.

43. Kuwajima, K., Mitani, M., and Sugai, S. (1989) *J. Mol. Biol. 206*, 547−561.
44. Yutani, K., Ogasahara, K., and Kuwajima, K. (1992) *J. Mol. Biol. 228*, 347−350.
45. Peng, Z., Wu, L. C., and Kim, P. S. (1995) *Biochemistry 34*, 3248−3252.
46. Creighton, T. E., and Ewbank, J. J. (1994) *Biochemistry 33*, 1534−1538.
47. Anfinsen, C. B., Haber, E., Sela, M., and White, F. H. (1961) *Proc. Natl. Acad. Sci. U.S.A. 47*, 1309−1314.
48. Shao, X., and Matthews, C. R. (1998) *Biochemistry 37*, 7850−7858.
49. Scheffzek, K., Ahmadian, M. R., Kabsch, W., Wiesmuller, L., Lautwein, A., Schmitz, F., and Wittinghofer, A. (1997) *Science 277*, 333−338.

BI9811157